Atomistic Modeling of Amorphous Polymer Bulk Based on an ab Initio Optimized Force Field

Bernd Kuhn,[†] Michael Ehrig, and Reinhart Ahlrichs*

Institut für Physikalische Chemie und Elektrochemie, Lehrstuhl für Theoretische Chemie, Universität Karlsruhe, Kaiserstr. 12, 76128 Karlsruhe, Germany

Received February 15, 1995; Revised Manuscript Received December 6, 1995[⊗]

ABSTRACT: In the present paper we introduce a new method to improve common force fields with respect to realistic modeling of the amorphous polymer bulk. To this end various force-field parameters are adjusted to results from ab initio calculations. Parameters for both intra- and intermolecular interactions are optimized for the first time using methods on an appropriate theoretical level. We derive a force field which is "tailor-made" for polypropylene and applicable to polypropylene chains of any tacticity. This new force field is used in subsequent molecular dynamics (MD) simulations of atactic polypropylene in a cubic box with periodic boundaries. We simulated an isothermal−isobaric (NpT) ensemble at $p = 1$ bar to predict characteristic bulk properties at temperatures above and below the glass point. Simulated densities and cohesive energies are in excellent agreement with experiment. Chain dimensions are characterized by the end-to-end distance and radius of gyration. The pair correlation function calculated for glassy atactic polypropylene confirms the complete absence of long-range order.

1. Introduction

The main interest in the theoretical modeling of polymers is concerned with the accurate prediction of specific physical and chemical properties. Most of the physical quantities which are important for the characterization of the polymer such as density, shape, and size of the chains[1] or elastic constants[2] are closely related to the solid-state structure of the bulk. The secondary structure of macromolecules is essentially determined by the folding of the chains. While bond lengths and bond angles differ little around their equilibrium values, dihedral angles assume the dominant role in the spatial configurations of polymers. In the following context we refer exclusively to the amorphous bulk. Methods that deal with crystalline polymers have been reported elsewhere.[3]

Since a realistic simulation of the polymer bulk structure implies the calculation of interactions between several hundred atoms, only methods of a lower theoretical level are applicable on today's computer hardware. In the present work we employed a molecular mechanics approach using the CFF91[4,5] force field which is implemented in the DISCOVER software package.[6] Force-field parameters for intermolecular interactions as well as parameters describing the torsional potential around the backbone atoms are of crucial importance for the purpose of predicting bulk properties. Generally these parameters are derived from results of quantum mechanical calculations on small model systems or fitted to a set of experimental data. Smith and Boyd[7] used spectroscopy results to optimize a force field for polymers containing ester groups. More recently Meier et al.[8] investigated the same polymer system but used semiempirical AM1 calculations on small polyester moieties as reference. Therefore informations about both barrier height and shape of the rotational potential could be made available. However, they scaled their relative AM1 energies by a factor of 1.9 to obtain good agreement with experimental gas-phase barriers. Yoon et al.[9] studied poly(vinyl chloride) melts by utilizing a force field with parameters obtained from ab initio calculations on 2,4-dichloropentane.

For the present work we enhanced the methods used so far for optimizing force-field parameters in two ways. At first torsional parameters were optimized with respect to the relative energies of a large number of rotational isomers. Due to the interdependence of neighboring dihedral angles ("pentane effect"[10]), we used a two-dimensional representation of the relative energies as a function of two consecutive backbone dihedrals as reference. This representation is also known as "$\phi-\psi$ map". Relative energies of the rotamers were calculated utilizing both semiempirical (AM1 Hamiltonian[11]) and ab initio (Hartree−Fock SCF[12]) methods. Our second modification concerned the optimization of the parameters describing nonbonded interactions. Optimizations of the nonbonded parameters for the purpose of realistic bulk modeling have rarely been published until now. Few approaches based the determination of nonbonded parameters on the dipole moments of small molecules.[7,9] Since a description of the intermolecular potential is crucial and experimental data are hardly available, a more reliable procedure appears desirable. We propose to use van der Waals parameters which are in agreement with the intermolecular pair potential of a small model system calculated with ab initio methods. Since the Hartree−Fock SCF method is not sufficient for the description of attractive dispersion effects, we applied calculations on a correlated level. An acceptable compromise between computational effort and quality of the results is the use of MP2[13] energies.

To demonstrate the capability of our method, we derive a force field which is "tailor-made" for polypropylene. This model polymer was selected because the description of the bonding situation does not cause severe problems and should therefore be described sufficiently well within the force field approximation. In addition, the presence of asymmetric centers in the vinyl chain allows the study of tacticity effects. We expect our method to be generally applicable to a variety of amorphous polymers.

One of the most important approaches in the prediction of polymer properties was introduced in the late 1960s by Flory[10] using statistical mechanics. Since this *rotational isomeric state* (*RIS*) model does not account

[†] Present address: Institut de Chemie Physique I, Département de Chimie, EPF Lausanne, 1015 Lausanne, Switzerland.

[⊗] Abstract published in *Advance ACS Abstracts,* May 1, 1996.

S0024-9297(95)00194-X CCC: $12.00

for intermolecular interactions, its application is limited to unperturbed chains in the gas phase. Nevertheless several structural properties of various polymes could be reproduced.[14−18] Theodorou and Suter[19] enhanced the RIS method through the invention of cubic periodic boundary conditions and consideration of intermolecular interactions. The bulk structure of glassy amorphous polymers was simulated by creating initial chain configurations in a stochastic process. This procedure, which is also called "amorphous cell construction", is followed by potential energy minimization. Structural properties and cohesive energy densities derived with this method for different amorphous polymers are in good agreement with the experiment.[19−21]

Using our optimized force field, we were interested in the prediction of properties of atactic polypropylene. The atactic form was chosen to ensure the bulk to be completely amorphous. To describe the bulk structure, we adopted some elements from Theodorou and Suter's procedure but improved their technique. First, we enlarged significantly the number of RIS states to generate more realistic starting structures. To take into account the influence of temperature, molecular dynamics (MD) simulations of the amorphous cell have been performed. The simulations were carried out in an isothermal−isobaric (NpT) ensemble at temperatures above and below the glass point of −18 °C ($p = 1$ atm).[22] Since the cell parameters are allowed to change during MD, we can compare the simulated density with experimental values. We give estimates for the cohesive energy density and the Hildebrand solubility parameter. The shape and size of the polymer chains are characterized by ensemble-averaged end-to-end distances and radii of gyration. Finally the local structure of the model system is characterized by a pair distribution function.

2. Methods

2.1. Force-Field Optimization. The CFF91 force field[4,5] is one of the second-generation (class II) force fields which are parametrized against a wide range of experimental and ab initio calculated data. It offers the possibility to use an extensive set of potential terms. In detail we have employed the following functional form:

bond stretching potential:

$$E_{\mathrm{str}} = \sum_a [K_{a,2}(r_a - r_a^0)^2 + K_{a,3}(r_a - r_a^0)^3 + K_{a,4}(r_a - r_a^0)^4] \quad (1)$$

Bond bending potential:

$$E_\theta = \sum_b [K_{b,2}(\Theta_b - \Theta_b^0)^2 + K_{b,3}(\Theta_b - \Theta_b^0)^3 + K_{b,4}(\Theta_b - \Theta_b^0)^4] \quad (2)$$

Torsional potential:

$$E_\phi = \sum_c \sum_{s=1}^{3} K_{c,s}[1 + \cos(s\Phi_c - \Phi_{c,s}^0)] \quad (3)$$

Sums are over all bond lengths a, bond angles b, and dihedral angles c. s denotes the expansion coefficient of the Fourier term. While K are the force constants, a superscript 0 indicates the expected equilibrium values.

Equation 4 illustrates the interaction potential between bond bending and torsion. The same polynomial structure also holds for all other cross terms:

$$E_{\theta,\phi} = \sum_b \sum_c \sum_{s=1}^{3} K_{b,c,s}[(\Theta_b - \Theta_b^0)(\cos(s\Phi_c - \Phi_{c,s}^0))] \quad (4)$$

Interactions between nonbonded atoms are represented by the following terms:

Coulombic potential:

$$E_{\mathrm{Coul}} = \sum_{i>j} q_i q_j / r_{ij} \quad (5)$$

van der Waals potential:

$$E_{\mathrm{vdW}} = \sum_{i>j} \sqrt{\epsilon(i)\,\epsilon(j)} \left[\frac{A_{ij}}{r_{ij}^{\,9}} - \frac{B_{ij}}{r_{ij}^{\,6}} \right] \quad (6)$$

where i and j run over all atoms. The van der Waals parameters—$\epsilon(i)$, A_{ij} and B_{ij}—describe both depth and shape of the Lennard-Jones potential. We used atomic charges q from different force fields and checked their reliability by means of population analyses[23−25] of the SCF wave function.

The total potential energy is evaluated by summing over all energy contributions:

$$E_{\mathrm{pot}} = E_{\mathrm{str}} + E_\theta + E_\phi + E_{\mathrm{str,str'}} + E_{\theta,\theta'} + E_{\mathrm{str},\theta} + E_{\mathrm{str},\phi} + E_{\theta,\phi} + E_{\theta,\phi,\phi'} + E_{\mathrm{Coul}} + E_{\mathrm{vdW}} \quad (7)$$

Within our work we successively optimized torsional parameters $K_{c,s}$ (eq 3) and then van der Waals parameters $\epsilon(i)$ (eq 6).

In the following we present a brief outline of the theoretical background of our procedure to determine potential parameters. By means of a least-squares fit, we minimized the variance S between relative energies of reference and force field structures with respect to the force field parameters x_i:

$$S = (1/n)\sum_{j=1}^{n} (\tilde{E}_j^{\mathrm{REF}} - \tilde{E}_j^{\mathrm{FF}})^2 \;!= \min \quad (8)$$

$$\Rightarrow \partial S/\partial x_i = 0 \;\forall\; i \quad (9)$$

$\tilde{E}^{\mathrm{REF}}$ and $\tilde{E}^{\mathrm{FF}}$ denote the reference and force field energies with respect to their arithmetic means and n is the number of reference structures. Introducing the Jacobian matrix $\mathbf{J}$, which is defined by

$$J_{jk} = \partial \tilde{E}_j^{\mathrm{FF}}(x^a)/\partial x_k \quad (10)$$

a simple transformation of the linear set of equations (9) yields the force-field parameter change $\Delta\mathbf{x}$:

$$\Delta\mathbf{x} = \mathbf{x}^{\mathrm{a}} - \mathbf{x} = [[\mathbf{J}(\mathbf{x}^{\mathrm{a}})]^{\mathrm{T}} \mathbf{J}(\mathbf{x}^{\mathrm{a}})]^{-1} \mathbf{J}(\mathbf{x}^{\mathrm{a}})[\tilde{\mathbf{E}}^{\mathrm{REF}} - \tilde{\mathbf{E}}^{\mathrm{FF}}(\mathbf{x}^{\mathrm{a}})] \quad (11)$$

$\mathbf{x}$ denotes the actual parameter set and $\mathbf{J}^{\mathrm{T}}$ is the transposed Jacobian. Since the minimization of S (eq 9) is an iterative procedure, we transform the expression above in a quasi-Newton algorithm[26] which permits faster convergence through successive improvement of

the Hessian matrix **H**:[27,28]

$$\Delta \mathbf{x} = -\mathbf{H}^{-1}\mathbf{g} \tag{12}$$

where the Hessian matrix satisfies

$$\mathbf{H}(\mathbf{x}^a) = (n/2)[\mathbf{J}(\mathbf{x}^a)]^T\mathbf{J}(\mathbf{x}^a) \tag{13}$$

and the gradient **g** is

$$\frac{\partial}{\partial \mathbf{x}} S(\mathbf{x}) = -\frac{2}{n}\mathbf{J}[\tilde{\mathbf{E}}^{REF} - \tilde{\mathbf{E}}^{FF}(\mathbf{x}^a)] \tag{14}$$

The torsional parameters of the force field were optimized with the following procedure assuming that the reference energies are already available (Their generation will be described later). In the first step force field structures and energies are calculated with parameters of the standard force field to obtain $\tilde{\mathbf{E}}^{FF}$. Reference conformations served thereby as starting structures. The next step yields **J** (eq 10), and so the gradient of the variance with respect to all force-field parameters x_i (eq 14). Jacobian matrix elements are calculated numerically by incrementation/decrementation of parameters. Although the just described procedure (to always consider the accurate conformer structures resulting from the current force-field parameters) is clearly preferable, it faces a problem. Local minima on the potential hypersurface may disappear or move considerably on slight variation of force field parameters which leads to numerical instabilities (This is a problem that cannot be avoided). In such a case we have decided not to relax the conformer geometry and used only the single-point energy in the regression.

The last step is concerned with the implementation of eq 12 and leads to a new parameter set which is employed in the subsequent optimization cycle. The parameters are considered to the optimal when changes of the mean-square deviation *S* (eq 8) and its gradient remain under a given threshold. The driver for this procedure which is depicted in Figure 1 was implemented using shell scripts and UNIX tools. van der Waals parameters were fitted in the same manner except that the force-field energies were calculated without preceding geometry optimizations. This is due to the fact that the van der Waals interactions depend on interatomic distances which are intermolecular in nature.

As mentioned above it is a useful approach to fit torsional parameters to the reference $\phi-\psi$ maps of small polymer moieties. A computer program, Surfer, was developed to evaluate these energy maps. To calculate the relative energies of the rotational isomers, we have employed the trimer 2,4,6-trimethylheptane, which is depicted in Figure 2. Dihedral angles ϕ and ψ of the two internal skeletal bonds were subsequently increased in fixed increments of 30° between 0° and 330°. This resulted in the computation of $12 \times 12 = 144$ reference energy values. The torsional angles were measured according to the nomenclature for vinyl polymer chains introduced by Flory et al.[29] (Figure 2). Semiempirical methods were used to optimize geometries for each rotational isomer whereby both relevant torsional angles were kept fixed. To this end we utilized the program MOPAC[30] with an AM1 parametrization. To reduce computational effort, the program Relax which is implemented in the program package TURBOMOLE[31] served as minimum searcher. We calculated single-point SCF energies with the TURBOMOLE program DSCF on the

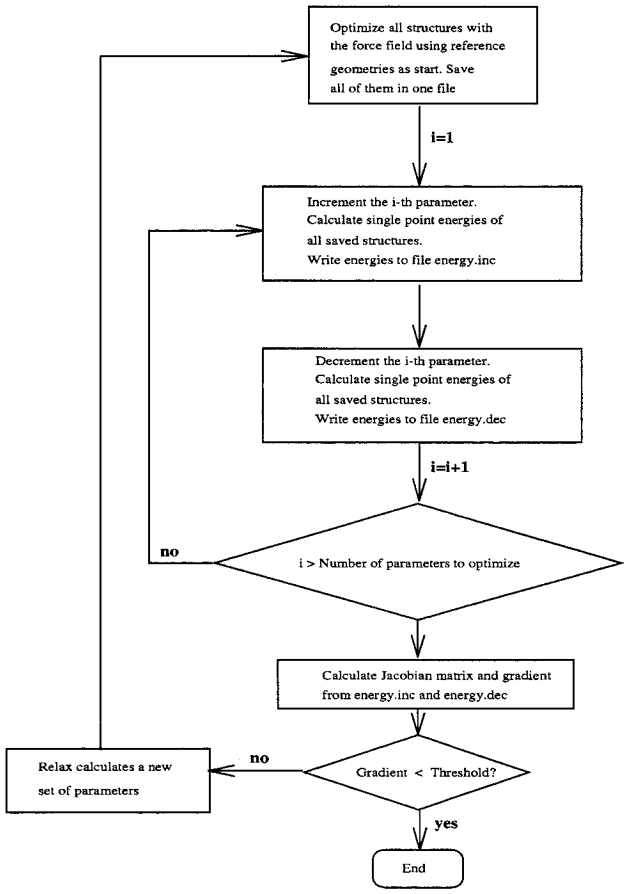

Figure 1. Flow chart diagram of the parameter fit procedure.

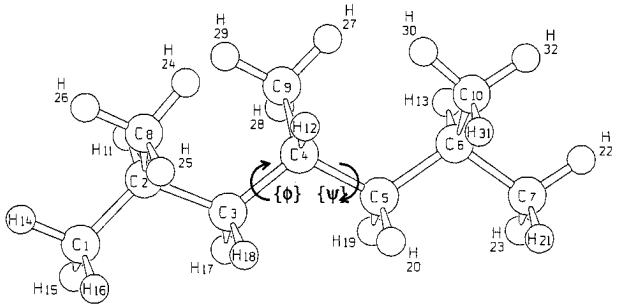

Figure 2. Structure and definition of torsional angles of the polypropylene chain.

Table 1. Atomic Basis Sets Used

Evaluation of $\phi-\psi$ Maps[32]		
C	(7s4p1d)/[3s2p1d]	$\eta_d = 0.8$
H	(4s1p)/[2s1p]	$\eta_p = 0.8$
Evaluation of Intermolecular Potential[32]		
(A) DZP		
C	(8s4p1d)/[4s2p1d]	$\eta_d = 0.8$
H	(4s1p)/[2s1p]	$\eta_p = 0.8$
(B) TZVDP[34]		
C	(11s6p2d)/[5s3p2d]	$\eta_d = 0.45, 1.4$
H	(5s2p)/[3s2p]	$\eta_p = 0.15, 1.0$

AM1-optimized structures. The basis sets used herein were of SVP[32] quality and are listed in Table 1. The quality of the Hartree−Fock SCF method was extensively investigated by Schäfer et al.[33] for small *n*-alkanes. Compared to methods which include correlation (MP2) the relative SCF energies of gauche conformations are clearly overestimated by a factor of 2−5 in those cases where the corresponding energy difference is small. To give an example: the energy

Table 2. Geometry Parameters for the Chain Construction Process

Bond lengths [Å]		Bond Angles (deg)	
C−C	1.54	C−C−C	109.5
C−H	1.07	C−C−H	109.5
		H−C−H	109.4

difference between the most stable conformer in *n*-pentane (trans−trans) is lower than the gauche−gauche form by 3.0 kcal/mol on the AM1/SCF level and 0.87 kcal/mol on the SCF/MP2 level.[33] For the energy-rich cis−cis conformer we compute relative energies (vs trans−trans) of 22.8 kcal/mol (AM1/SCF), 18.9 kcal/mol (SCF/SCF) and 17.8 kcal/mol (SCF/MP2) with a large triple-ζ valence double polarization basis.[34] We are aware of this shortcoming, but geometry optimizations on MP2 level to calculate a complete $\phi-\psi$ map are not feasible since they are too time-consuming. To check the influence of chain size and tacticity torsional parameters were additionally derived for several tetrameric oligomers and compared with the trimer values. The tetramers differed in the chirality of the skeletal bonds and in the central chain segment ([$-CH_2-$] respectively [$-CH(CH_3)-$]).

For a realistic simulation of the bulk properties, it is essential to optimize van der Waals parameters because of their outstanding importance for intermolecular interactions. In bulklike polypropylene these interactions are dominated by the forces between hydrogen atoms. Therefore we used a methane dimer as model system and fitted the van der Waals parameters to the MP2 calculated intermolecular potential. The size of the system considered (the CH_4 dimer) is limited by the restriction that the calculation time for MP2 energies scales with the fifth power with the number of basis functions and other systems were not tractable (by us). Furthermore, a reliable fitting procedure implies the calculation of a large number of reference values. In this work we probed the intermolecular pair potential of the dimer between 6 and 10 au (distance between carbons) in fixed increments of 0.1 au. Taking into account four different configurations for each distance resulted in a total of 164 reference energies. Since the results of correlated calculations strongly depend on the applied basis set we used both DZP[32] and TZVDP[32] basis sets and estimated the basis-set superposition error (BSSE) by the counterpoise correction procedure[35] for the latter basis. Contraction schemes and exponents of the polarization functions are given in Table 1.

2.2. Modeling of the Amorphous Bulk. To simulate the solid-state structure of atactic polypropylene, we applied a two-stage approach. The first step comprised the generation of initial configurations with the method invented by Suter et al.[19] The starting structures were relaxed afterward by means of MD calculations to a state of thermodynamical equilibrium. To perform the computation in a reasonable time we limited the chain length to 76 monomeric units.

At the onset a cubic box with a volume defined by the polymerization degree and a given initial density was calculated. The polypropylene chain was generated using a modified Markov process in a bond-by-bond manner. On the basis of the calculated $\phi-\psi$ maps, we constructed statistical weight matrixes with 16 RIS states and compared the results with Flory's five-state scheme used so far.[14,19] Table 2 shows bond lengths and bond angles which were used in the construction process. The fraction of meso dyads in a polypropylene chain is assumed to be 48%.[36] Bulk effects are taken into consideration by interactions between chain segments of mirror images of the "parent chain".

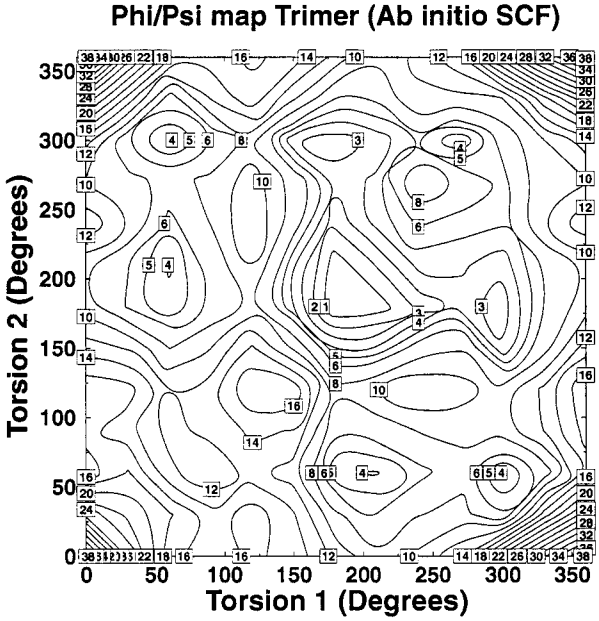

Figure 3. $\phi-\psi$ map of the trimer 2,4,6-trimethylheptane (ab initio SCF). Torsional angles 1 and 2 denote both fixed C−C−C−C-torsions ϕ and ψ of the trimer. Energy values in the contour diagram are in kcal/mol.

The starting structures were refined to thermodynamical equilibrium with the following relaxation strategy: (i) 500 cycles potential energy minimization with respect to all internal degrees of freedom. (ii) MD simulation on a constant-temperature, constant-pressure ensemble at $T = 233$ K and $T = 298$ K ($p = 1$ bar) using Berendsen's method.[37] For each structure a dynamics run of 30 ps was performed. The time step for the integration of Newton's equations of motion was 1 fs. To increase computational efficiency, interactions between nonbonded atoms were only calculated within a "cutoff" of 8.0 Å in its full strength. A quintic spline between 8.0 and 8.5 Å was used to prevent truncation errors. The effect of neglecting nonbonded interactions between atoms with distances larger than the "cutoff" radius was checked.

Construction and relaxation of the amorphous cell have been carried out on 10 different configurations. In the property finding process we calculated MD trajectories for the duration of 10 ps for each cell. Snapshots were taken every 1 ps to average over thermal vibrations which yielded a total amount of 100 different model structures.

3. Results

3.1. Torsional Parameter Fit. Let us stress again that although the torsional profiles computed on the SCF level are clearly not exact they are the best compromise between computational effort and accuracy. Torsional parameters were fitted to the relative ab initio SCF energies of the trimer. The force field so obtained will be denoted as "torsopt" throughout. Figure 3 shows the two-dimensional reference energy contour diagram of this moiety as a function of the torsional angles ϕ and ψ marked in Figure 2. Since the substituents of the atoms defining the fixed torsions are identical, the $\phi-\psi$ map shows corresponding symmetry. The rotational barrier of the skeletal chain bonds in polypropy-

Table 3. Comparison of MOPAC and Force-Field Methods for Different Tetramers[a]

	[CH$_2$][c]		[CH(CH3)][c]	
method	isotactic[b]	syndiotactic[b]	isotactic[b]	syndiotactic[b]
MOPAC	1.96	1.81	2.19	2.25
MOPAC (scaled)[d]	2.72	2.77	2.33	2.36
CFF91 ("standard")	2.43	2.41	2.83	2.73

[a] Numerical values denote the root-mean-square deviation (eq 8) to the relative ab initio SCF energies in kcal/mol. [b] Tacticity of the skeletal bonds. [c] Central chain segment. [d] Scaling factor 2.0.

Table 4. Force-Field Charges in Comparison with Results from Population Analyses

atom type	CFF91	CVFF	Mulliken	Roby−Davidson
H	0.053	0.100	0.0 to 0.1	0.0 to 0.05
C1[a]	−0.053	−0.100	−0.3 to 0.0	−0.1 to 0.0
C2[a]	−0.106	−0.200	−0.3 to 0.0	−0.1 to 0.0
C3[a]	−0.159	−0.300	−0.3 to 0.0	−0.1 to 0.0

[a] Different carbon atom types corresponding to the number of connected hydrogen atoms.

lene is 3-fold because of the sp^3 hybridization of all carbon atoms. All nine minima which should be expected in this first-order approximation can be located.

Geometry optimization on the semiempirical level provided us with AM1 energies for all rotational isomers. To test the reliability of these energies, we calculated the root-mean-square deviation (eq 8) to the relative ab initio energies of four different tetramers. Table 3 shows that AM1 energies are merely 18−25% better than CFF91 force-field energies when using standard parametrization. Coussens et al.[38] scaled AM1 energies with a factor of 1.9 and obtained good agreement with experimental rotational barriers for aromatic polyester moieties. By contrast our scaled results show even poorer agreement with ab initio data than the unscaled values (5−53%). Hence this procedure appears to be not generally applicable.

Before we started to fit the torsional parameters, the influence of different atomic charges on the relative energies of the rotamers was tested. Calculations were carried out with CFF91 charges, CVFF[39] charges, and without electrostatic interactions. The atomic charge values are given in Table 4. A total neglect of Coulombic interactions increased the root mean square deviation by less than 5%. This fact is not surprising since all bonds in polypropylene are of little polarity. The standard deviation was least with CVFF charges which were therefore adopted for all further calculations. Population analyses have been performed to verify the CVFF values. Both Mulliken[23] and Roby−Davidson[24,25] methods confirm the force-field charges in sign and size (Table 4).

Polypropylene has three torsions with different parametrization, namely, C−C−C−C, C−C−C−H and H−C−C−H. Since the applied torsional potential contained 1-, 2-, and 3-fold torsion terms each, we fitted a total of nine dihedral parameters. Our fit procedure improved the standard deviation from 2.49 to 1.57 kcal/mol. Table 5 lists all optimized torsional force-field parameters. A comparison between the $\phi-\psi$ map obtained with the "torsopt" force field (Figure 4) and the reference energy map (Figure 3) gives a first impression of the quality of our newly derived torsional parameters. To quantify the comparison, we fitted a two-dimensional, quadratic trial function to all minima of both $\phi-\psi$ maps. These results and the values obtained with standard parametrization are given in Table 6, which contains locations and relative energies as well as standard deviations between energy map and test function.

Table 5. Optimized Torsional Parameters[a]

type of torsion	Fourier expansion coefficient[b]	original parameter kcal/mol	optimized parameter kcal/mol	σ_n[c] kcal/mol
C−C−C−C	1	0.122	3.595	1.57
C−C−C−C	2	0.051	−3.018	
C−C−C−C	3	−0.223	0.076	
H−C−C−C	1	0.000	0.264	
H−C−C−C	2	0.032	−0.757	
H−C−C−C	3	−0.178	−0.704	
H−C−C−H	1	−0.243	−3.891	
H−C−C−H	2	0.062	1.889	
H−C−C−H	3	−0.138	0.551	

[a] CVFF charges were used during the fit procedure. [b] See eq 3. [c] Root-mean-square between force field and ab initio energies. σ_n for standard parametrization is 2.49 kcal/mol.

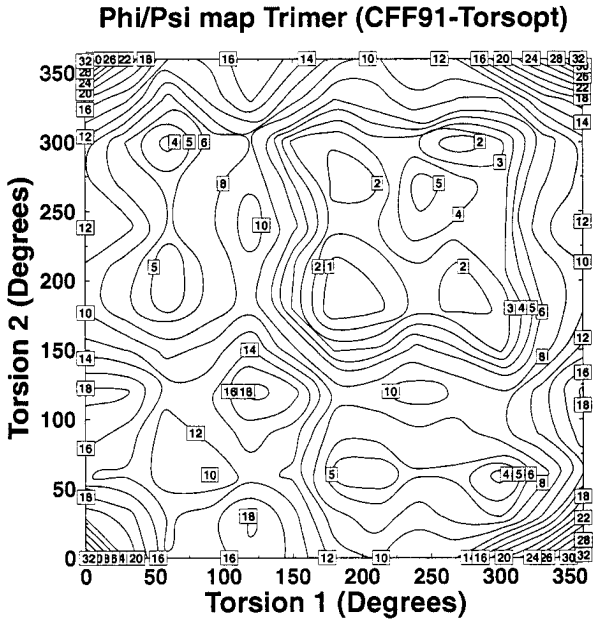

Figure 4. $\phi-\psi$ map of the trimer 2,4,6-trimethylheptane (CFF91 with optimized torsional parameters). For an explanation of the contour diagram, see Figure 3.

The shapes of the potential wells are characterized by eigenvalues of the force constant matrix with respect to ϕ and ψ. The energetic differences of the minima calculated with the standard force field (CFF91) to the reference values are significant. Generally the relative energies of all minima are too low by a factor of 1.5. The most important improvement through our optimization procedure results in a more realistic description of the $\phi-\psi$ map. The energetic differences between reference and "torsopt" force field minima are within 0.9 kcal/mol with a single exception concerning the 300°/300° conformation (Table 6). Corresponding calculations for the tetramers corroborate the results for the trimer and show even poorer results for the standard force field. The highest-lying conformation was underestimated by a factor of 2 as compared to the ab initio energy.

To verify the physical justification of the optimized torsional parameters, we compared structures obtained with the standard and "torsopt" force field using the corresponding semiempirical geometries as reference. Table 7 lists root-mean-squares and mean deviation for several torsional and valence angles. The structures calculated with the "torsopt" parameter set show better agreement with reference structures than using the

Table 6. Comparison of $\phi-\psi$ Map Minima for Different Force Fields

minimum[a]					
ϕ_{min}	ψ_{min}	E_{rel},[a] kJ/mol	k_1,[a] kJ/rad^2	k_2,[a] kJ/rad^2	σ_n,[b] kJ
		Ab Initio SCF			
189.2	189.2	0.00	22.2	16.0	0.05
189.2	295.2	2.81	9.2	20.9	0.21
60.5	292.5	4.05	33.7	24.6	0.53
61.6	204.0	4.53	20.3	8.1	0.11
294.1	278.8	4.87	27.3	7.3	0.28
71.8	83.4	11.09	22.2	11.7	0.19
		CFF91 "Torsopt"			
190.4	190.4	0.00	18.2	15.3	0.03
292.7	285.7	2.07	29.0	5.4	0.18
185.3	280.7	2.18	13.9	2.1	0.14
57.6	288.1	4.00	26.3	17.5	0.31
63.6	204.9	4.52	20.1	9.1	0.11
67.1	58.4	10.22	21.3	6.3	0.20
		CFF91 "Standard"			
185.9	185.9	0.00	20.4	17.1	0.03
295.5	283.4	1.98	23.7	12.3	0.21
169.6	317.1	2.14	15.9	1.9	0.16
61.4	193.1	2.74	15.4	21.4	0.09
53.2	297.2	2.94	18.9	13.4	0.27
65.0	59.0	7.13	17.6	2.9	0.26

[a] Minima, relative energies (E_{rel} and eigenvalues of the force constant matrix (k_1, k_2) were derived from the test function: $E(\phi,\psi) = E(\phi_{min}, \psi_{min}) + c(\phi - \phi_{min})^2 + d(\psi - \psi_{min})^2 + e(\phi - \phi_{min})(\psi - \psi_{min})$. Number of fitting points for each minimum: 9. [b] Standard deviation between $\phi-\psi$ map energies and test function.

Table 7. Comparison of Geometries Obtained with "Standard" and "Torsopt" Force Field[a]

internal coordinate	"standard"	"torsopt"
	Torsional Angle	
C1−C2−C3−C4[b]	16.48 (+9.0)	13.36 (+4.6)
C4−C5−C6−C7[b]	16.47 (−4.5)	12.32 (−2.3)
C5−C6−C7−H22[b]	6.98 (−0.1)	7.18 (−2.2)
	Valence Angle	
C1−C2−C3[b]	1.27 (−0.5)	0.99 (−0.1)
C2−C3−C4[b]	3.85 (+3.7)	4.01 (+3.9)
C3−C4−C5[b]	1.27 (+0.8)	1.08 (+0.5)

[a] Numerical values denote the root-mean-square and mean deviation (in parentheses), respectively, between force-field structural parameters and semiempirical reference values. Mean values are over 144 rotamers. [b] The numbering of the atoms refers to Figure 2.

Table 8. Comparison of Force Fields for Different Tetramers[a]

	[CH2][c]		[CH(CH3)][c]	
method	isotactic[b]	syndiotactic[b]	isotactic[b]	syndiotactic[b]
CFF91 ("standard")	2.12	2.16	2.52	2.50
CFF91 ("torsopt")[d]	1.31	1.23	1.73	1.82
tetramer−optim[e]			1.62	1.76

[a] Numerical values denote the root mean square deviation (eq 8) to the relative ab initio energies in kcal/mol. All values were calculated with CVFF charges. [b] Tacticity of the skeletal bonds. [c] Central chain segment. [d] Optimized torsional parameters for the trimer. [e] Optimized torsional parameters for [CH(CH3)] tetramers.

standard parametrization. This is not unexpected; it has to be noted however that only torsional parameters were adjusted.

The new force field was derived on the premise of being appropriate for polypropylene chains of any tacticity. We tested the transferability of the "torsopt" force field on four tetramers. Table 8 illustrates that the improvement in the standard deviation obtained with the "torsopt" parameter set is similar (27−43% vs 37%) to the trimer value. Further optimization cycles on iso- and syndiotactic tetramers including all nine torsional parameters reveal that optimizations on tetrameric chain portions improve the root-mean-square deviation

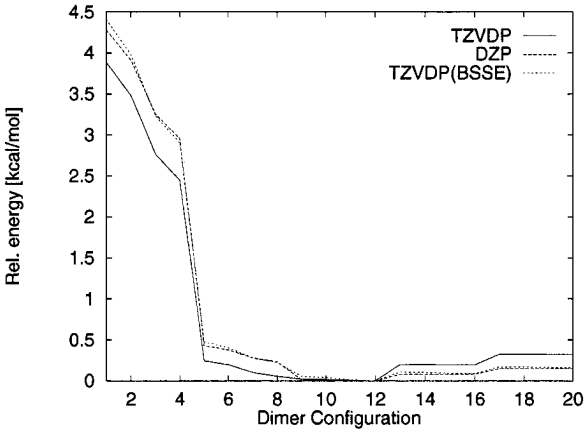

Figure 5. Relative MP2 energies for $(CH_4)_2$ as obtained with different basis sets.

Table 9. Optimized van der Waals Parameters[a]

parameter type	original parameter, kcal/mol	optimized parameter, kcal/mol	σ_n,[a] kcal/mol
$\epsilon(C)$	0.0540	0.1589	0.128
$\epsilon(H)$	0.0200	0.0177	

[a] CVFF charges were used during the fit procedure. [b] Root-mean-square deviation between force field and MP2 energies. σ_n for standard parametrization with optimized torsional parameters is 0.281 kcal/mol.

merely by 0.1 kcal/mol. We can conclude that the torsional parameters fitted for the trimer are universally applicable to all polypropylenes.

3.2. Van der Waals Parameter Fit. MP2 calculations on the model system $(CH_4)_2$ for optimization of the van der Waals parameters $\epsilon(i)$ (eq 6) for carbon and hydrogen were carried out with DZP and TZVDP basis sets. Since the relative energies for the methane dimer differed markedly, we investigated the effect of BSSE and corrected the TZVDP values. Figure 5 illustrates for 20 selected dimer configurations the behavior of the relative energies for DZP, TZVDP, and TZVDP(BSSE), i.e., TZVDP corrected for the BSSE. To our surprise, we found a nearly perfect correspondence between the TZVDP(BSSE) and the DZP values. Obviously, there is a consistent error compensation in this case. Due to this fact we fitted the van der Waals parameters for the large number of reference structures to the intermolecular pair potential obtained with the DZP basis set. The force field resulting from the optimization of torsional parameters and van der Waals parameters (as just described) will be denoted as "fullopt". Optimal van der Waals parameters for carbon and hydrogen are assembled in Table 9. Our parameter optimization reduced the root-mean-square deviation (eq 8) by 54% (0.281 kcal/mol (standard CFF91) vs 0.128 kcal/mol. Figure 6 demonstrates the good agreement between reference (MP2) and "fullopt" force-field energies.

3.3. Generation and Relaxation of the Amorphous Cell. In the first step of the bulk simulation of atactic polypropylene, we had to construct an amorphous cell. Since we employed an initial density of 0.7 g/cm^3, our model cube at the beginning had edges 19.65 Å long and was filled with a total of 686 interacting atoms. To avoid surface effects, the cube was surrounded on all sides by 26 identical copies. While Suter et al.[19] used the five-state model in the construction process, we allowed 16 RIS states. These values were derived from ab initio calculated $\phi-\psi$ maps of the tetramers. Our enhancement decreased the initial energy of the amorphous cell by 2 orders of magnitude

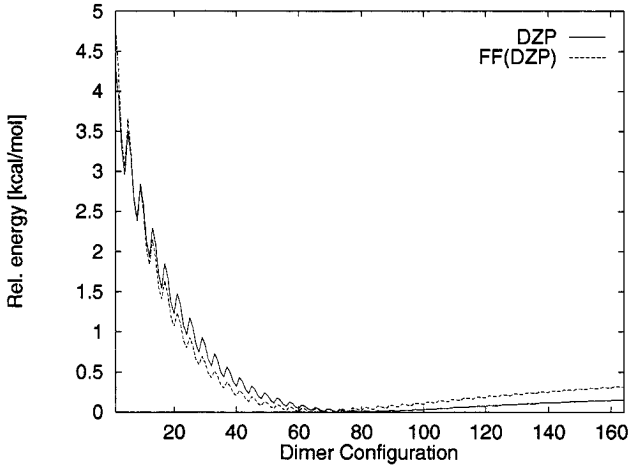

Figure 6. Relative MP2 reference energies obtained with the DZP basis set in comparison with the CFF91 "fullopt" force field values FF(DZP).

Table 10. Simulated Densities of Atactic Polypropylene with Different Force Fields for Systems of Parent Chains of 76 Monomers[a]

force field	$T = 233$ K[b]	$T = 298$ K[b]
"standard"	0.76 ± 0.02	0.74 ± 0.02
"torsopt"	0.78 ± 0.02	0.76 ± 0.02
"fullopt"	0.86 ± 0.02	0.85 ± 0.01
experiment	0.89[22]	0.85[40]

[a] Densities were averaged over 100 model structures each. Mean densities and corresponding standard deviations are given in g/cm^3. [b] $p = 1$ bar.

(10^6-10^7 kcal/mol for 5 RIS states vs 10^4-10^5 kcal/mol for 16 RIS states). Nevertheless we could not find any difference in the simulated density after molecular dynamics calculations for both RIS approaches. During the MD simulations with our "fullopt" force-field 23% of all skeletal torsions changed their values by more than 60°. This is somewhat less than using CFF91 standard parametrization (32%) which is consistent with the fact that the rotational barrier is significantly increased with optimized torsional parameters. We conclude that MD simulations are the most important part in the modeling procedure whereby the density is relatively independent of the initial guess structure.

Artifacts in the simulation of solid-state structures may occur if the size of the periodic cell or the "cutoff" for nonbonded interactions are too small. To investigate the influence of these potential errors we varied the chain length to a polymerization degree $x = 500$ and increased the "cutoff" up to 16.5 Å using the method described above. The mean density of 30 model structures differed at most by 1% from the cell containing chains with $x = 76$ using a "cutoff" radius of 8.5 Å. This excellent agreement is a justification to limit the chain length to 76 monomeric units and the "cutoff" to 8.5 Å.

Density. Since the density is an important property of polymers and can be easily determined in experiments, we focused our attention on the computation of the bulk density. Table 10 shows results for the simulation obtained with the CFF91 force field using different parametrization at 233 and 298 K ($p = 1$ bar). Since the simulated densities represent mean values of 100 different model structures, standard deviations are given to characterize the statistical uncertainty. Experimental densities are 0.89[22] and 0.85[40] g/cm^3 at $T =$ 233 and 298 K, respectively. The present results show that the optimization of nonbonded parameters is of outstanding importance for a realistic prediction of the bulk density. Densities computed with standard parametrization are about 0.1 g/cm^3 too low, they can be improved by 0.02 g/cm^3 through the use of fitted torsional parameters which is clearly unsatisfactory. Only when van der Waals parameters were optimized in addition the computed density improves drastically: within the statistical deviation there is a nearly perfect correspondence for both temperatures between the "fullopt" force field density (0.86 and 0.85 g/cm^3 at $T =$ 233 and 298 K, respectively) and the experimental values.

To test the general applicability of out "fullopt" force field to polypropylenes of different stereochemical configuration, we computed the mean density for 10 different configurations of isotactic samples ($x = 76$) at 298 K ($p = 1$ bar). Since our simulation procedure is restricted to amorphous polymers, we can predict only the density of the amorphous part of isotactic polypropylene which is semicrystalline as a whole. The experimental value for the amorphous region obtained from extrapolation of densities above the melting point is 0.85 g/cm^3.[41] As with atactic polypropylene, we obtained very satisfactory results with our fully optimized force field. The simulated density with standard parametrization (0.74 ± 0.02 g/cm^3) was improved to 0.84 ± 0.03 g/cm^3 with the "fullopt" force field.

Table 11. Comparison of Cohesive Energy Densities E_{coh} and Hildebrand Solubility Parameters δ[a]

method	E_{coh}, J/m^3	δ, $\sqrt{\text{J/cm}^3}$
"standard"	$(1.6 \pm 0.2) \times 10^8$	12.7 ± 0.8
"fullopt"	$(4.0 \pm 0.4) \times 10^8$	19.9 ± 1.0
Suter et al.[19]	$(2.0 \pm 0.2) \times 10^8$	14.2 ± 0.8
experiment[40]	$(2.83-3.54) \times 10^8$	$16.8-18.8$

[a] Calculated properties are for atactic polypropylene ($x = 76$) at $T = 298$ K and $p = 1$ bar. We averaged our theoretical values over 100 model structures each.

Cohesive Energy Density. The cohesive energy density of a substance E_{coh}, which is defined as the intermolecular part of the internal energy U per mole of substance, is a common quantity in the characterization of polymer mixture systems. The cohesive energy density corresponds to the cohesive energy per unit volume. E_{coh} is calculated as an ensemble average of the expression

$$E_{coh} = U_{intra} - U_{tot} \tag{15}$$

where U_{intra} is the intramolecular energy of the parent chain and U_{tot} denotes the total internal energy. Alternatively, experimentalists often use the Hildebrand solubility parameter which is the square root of E_{coh}. For the atactic form ($x = 76$) we have computed cohesive energy densities and Hildebrand parameters for an ensemble of 100 model structures at $T = 298$ K and $p = 1$ bar (see Table 11). Experimental values[40] for polypropylene are available but without any tacticity specified. The predictions of Suter et al.[19] using the same chain length in their simulation are on the lower edge of the experimental results, whereas the "fullopt" force field slightly overestimates the solubility parameter. Nevertheless, it still ranges within the statistical error. Using the standard force field yields theoretical values which are obviously too low.

Chain Dimensions. Size and shape of the polymer chains are frequently characterized by ensemble averages of the end-to-end distance $\sqrt{\langle r^2 \rangle}$ and radius of

Table 12. Comparison of End-to-End Distances and Radii of Gyration[a]

method	$\sqrt{\langle r^2 \rangle}$ [Å]	$\sqrt{\langle s^2 \rangle}$ [Å]	$\sqrt{\langle s^2 \rangle}$ [Å]
x[b]	76	76	500
"standard"	45.6 ± 3.9	17.5 ± 0.8	29.2 ± 1.1
"fullopt"	32.8 ± 7.1	13.9 ± 1.1	29.9 ± 1.9
Suter et al.[19]	40.1 ± 3.2	17.2 ± 1.1	
RIS values[19]	47.0 ± 0.1	18.8 ± 0.1	
experiment[42]			49.9 ± 0.4

[a] Calculated properties are for atactic polypropylene at $T = 233$ K and $p = 1$ bar. We averaged our theoretical values over 100 ($x = 76$) respectively 30 ($x = 500$) model structures. [b] x = polymerization degree.

gyration $\sqrt{\langle s^2 \rangle}$. In our calculations both parameters have been averaged over 100 different model structures for the atactic form ($x = 76$) at $T = 233$ K and $p = 1$ bar which are assembled in Table 12. There is a remarkable difference in the theoretical prediction between both force fields. Using our optimized parametrization, the chains seem to be more compact compared to the standard force fields results. Suter et al.[19] performed calculations on atactic polypropylene chains with the same fraction of meso dyads and polymerization degree but averaged over 15 amorphous cells. Additionally they computed RIS values from 100 Bernoullian configurations for the same chain length. The RIS assumption of unperturbed chains is very poor leading to the highest values in the end-to-end distance and radius of gyration. They are decreased slightly when employing the standard force field. While $\sqrt{\langle r^2 \rangle}$ obtained with Suter's polypropylene specific force field is significantly decreased $\sqrt{\langle s^2 \rangle}$ remains virtually identical. Our estimates with the "fullopt" parametrization are about 25% smaller than the results from Suter et al. Since the radius of gyration strongly depends on the polymerization degree (x) and experimental values are only available for $x \approx 500$ we additionally evaluated $\sqrt{\langle s^2 \rangle}$ for 30 model structures with $x = 500$. In contrast to the results for the shorter chain, there is virtually no difference between both force fields. Both values are too low by a factor of 2 compared to the experiment.

Pair Correlation Function. The distribution of the atoms in the amorphous cell have been characterized by a pair correlation function $g(r)$ for glassy atactic polypropylene at $T = 233$ K. To minimize the statistical error we calculated $g(r)$ for a cell containing 1000 skeletal bonds ($x = 500$). Since the interatomic HH distances are of great importance for the bulk density, we discuss the radial distribution function for hydrogen atoms. $g_{HH}(r)$, and its intermolecular part for the "fullopt" force field are depicted in Figure 7. Sharp peaks in the total correlation function are due to the bonding situation, e.g., the first peak at 1.8 Å represents the distance of hydrogens located at the same carbon atom. As expected for an amorphous system, no long-range order can be observed. The intermolecular part of $g_{HH}(r)$ is almost structureless. Only a shoulder between 2.2 and 2.7 Å can be determined. This distance range is approximately the sum of the van der Waals radii of two hydrogen atoms.

3.4. Computational Efforts. Ab initio calculations of the reference energies as well as the optimization of the force field parameters have been carried out on workstations IBM RS6000/360. The evaluation of a reference $\phi-\psi$ map with 144 points lasted 12 days. The calculation of the 164 MP2 reference energies for the methane dimer using the large TZVDP basis set took about 6 days. While the optimization of all nine torsional parameters required a total of 10 h, this work was done within 1 h for the van der Waals parameters. Construction and relaxation of the amorphous cell have been performed on an IRIS Indigo R4000 workstation. The MD simulation for each configuration ($x = 76$) took 6 h.

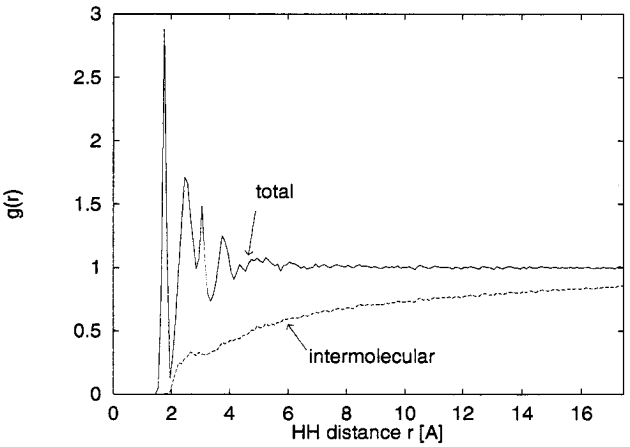

Figure 7. Computed hydrogen−hydrogen pair correlation function of the amorphous cell of polypropylene.

4. Conclusions

The aim of our work was to optimize a widely used and commercially available force field (CFF91[4,5]) with the purpose of using it in the realistic modeling of the bulk structure for specific kinds of amorphous polymers. We used polypropylene as a test case for our fitting procedure. Nevertheless, the software designed by us can be applied without problems to other polymer systems and force fields. In the fitting procedure both torsional and van der Waals parameters have been optimized with respect to the relative energies of various polymer configurations utilizing ab initio energies as reference. We considered the correct prediction of the density as a criterion for the quality of our force field. The optimization of the CFF91 torsional parameters improved the density from 0.74 ± 0.02 to 0.76 ± 0.02 g/cm^3 ($T = 298$ K). Fundamental progress could be made through optimization of the van der Waals parameters. The value of 0.85 ± 0.01 g/cm^3, at $T = 298$ K, is in full agreement with the experiment (0.85 g/cm^3).[40] The analogous simulation for a temperature ($T = 233$ K) below the glass point of $T = 255$ K ($p = 1$ atm)[22] resulted in a comparably good agreement with experiment. Our improvements made in the prediction of the density carry over to other properties. The computed cohesive energy density and the Hildebrand parameter are in very good agreement with experiment too (within the limits of uncertainties). No improvement was obtained for the simulation of the radius of gyration. The pair correlation function evaluated for HH distances shows all characteristic features of an amorphous substance.

We expect that the developed force field yields comparably good results in the prediction of other properties of amorphous polypropylene, e.g., X-ray and neutron-scattering curves or elastic constants. The correct prediction of the glass transition behavior provides a further test of the optimized parameter set.

Acknowledgment. We gratefully thank Dr. O. Evers and Dr. E. Hädicke for helpful discussions. This work was supported financially by the BASF AG and the Fonds der Chemischen Industrie.

References and Notes

(1) Theodorou, D. N.; Suter, U. W. *Macromolecules* **1985**, *18*, 1206.
(2) Theodorou, D. N.; Suter, U. W. *Macromolecules* **1986**, *19*, 139.
(3) Sorensen, R. A.; Liau, W. B.; Boyd, R. H. *Macromolecules* **1988**, *21*, 194.
(4) Maple, J.; Dinur, U.; Hagler, A. T. *Proc. Natl. Acad. Sci. U.S.A* **1988**, *85*, 5350.
(5) Maple, J.; Thacher, T. S.; Dinur, U.; Hagler, A. T. *Chem. Design Automat. News* **1990**, *5*(9), 5.
(6) Discover User Guide, Parts 1−3, version 2.9/3.1 Biosym Technologies: San Diego, 1993.
(7) Smith, G. D.; Boyd, R. H. *Macromolecules* **1990**, *23*, 1527.
(8) van Ruiten, J.; Meier, R. J.; Hahn, C.; Mosell, T.; Sariban, A.; Brickmann, J. *Macromolecules* **1993**, *26*, 1555.
(9) Smith, G. D.; Jaffe, R. L.; Yoon, D. Y. *Macromolecules* **1993**, *26*, 298.
(10) Flory, P. J. *Statistical Mechanics of Chain Molecules*; Wiley-Interscience: New York, 1969.
(11) Dewar, M. J. S.; Zoebisch, E. G.; Healy, E. F.; Stewart, J. J. P. *J. Am. Chem. Soc.* **1985**, *107*, 3902.
(12) Szabo, A.; Ostlund, N. S. *Modern Quantum Chemistry*; McGraw-Hill: New York, 1989.
(13) Møller, C.; Plesset, M. S. *Phys. Rev.* **1934**, *46*, 618.
(14) Suter, U. W.; Flory, P. J. *Macromolecules* **1975**, *8*, 765.
(15) Yoon, D. Y.; Sundararajan, P. R.; Flory, P. J. *Macromolecules* **1975**, *8*, 776.
(16) Tonelli, A. E. *Polymer* **1982**, *23*, 676.
(17) Lee, K. J.; Mattice, W. L. *Comput. Polym. Sci.* **1991**, *1*, 213.
(18) Tarazona, M. P.; Saiz, E.; Gargallo, L.; Radic, D. *Makromol. Chem., Theory Simul.* **1993**, *2*, 697.
(19) Theodorou, D. N.; Suter, U. W. *Macromolecules* **1985**, *18*, 1467.
(20) Hutnik, M.; Argon, A. S.; Gentile, F. T.; Ludovice, P. J.; Suter, U. W. *Macromolecules* **1991**, *24*, 5962.
(21) Ludovice, P. J.; Suter, U. W. *Plast. Eng. (Comput. Model. Polym.)* **1992**, *25*, 161.
(22) Kaufmann, H. S.; Falcetta, J. J. *Introduction to Polymer Science and Technology*; Wiley-Interscience: New York, 1977.
(23) Mulliken, R. S. *J. Chem. Phys.* **1955**, *23*, 1833.
(24) Roby, K. R. *Mol. Phys.* **1974**, *27*, 81.
(25) Davidson, E. R. *J. Chem. Phys.* **1967**, *46*, 3320.
(26) Press, W. H.; Flannery, B. P.; Teukolsky, S. A.; Vetterling, W. T. *Numerical Recipies*: Cambridge University Press: Cambridge, 1988, Chapter 10.
(27) Broyden, C. G. *J. Instrum. Math. Appl.* **1970**, *6*, 76. Fletcher, R. *Comput. J.* **1970**, *13*, 317. Goldfarb, D. *Math. Comput.* **1970**, *24*, 23. Shanno, D. F. *Math. Comput.* **1970**, *24*, 647.
(28) Császár, P.; Pulay, P. *J. Mol. Struct.* **1984**, *114*, 31.
(29) Flory, P. J.; Sundararajan, P. R.; DeBolt, L. C. *J. Am. Chem. Soc.* **1974**, *96*, 5015.
(30) Dewar, M. J. S. *J. Mol. Struct.* **1983**, *100*, 41.
(31) Ahlrichs, R.; Bär, M.; Häser, M.; Horn, H.; Kölmel, C. *Chem. Phys. Lett.* **1989**, *162*, 165.
(32) Schäfer, A.; Horn, H.; Ahlrichs, R. *J. Chem. Phys.* **1992**, *97*, 2571.
(33) Frey, R. F.; Cao, M.; Newton, S. Q.; Schäfer, L. *J. Mol. Struct. (THEOCHEM)* **1993**, *285*, 99.
(34) Schäfer, A.; Huber, C.; Ahlrichs, R. *J. Chem. Phys.* **1994**, *100*, 5829.
(35) Hobza, P.; Zahradnik, R. *Chem. Rev.* **1988**, *88*, 871.
(36) Suter, U. W.; Neuenschwander, P. *Macromolecules* **1981**, *14*, 528.
(37) Berendsen, H. J. C.; Postma, J. P. M.; van Gunsteren, W. F.; Dinola, A.; Haak, J. R. *J. Chem. Phys.* **1984**, *81*, 3684.
(38) Coussens, B.; Pierloot, K.; Meier, R. J. *J. Mol. Struct. (THEOCHEM)* **1992**, *91*, 331.
(39) Dauber-Osguthorpe, P.; Roberts, V. A.; Osguthorpe, D. J.; Wolff, J.; Genest, M.; Hagler, A. T. *Proteins: Struct., Function Genet.* **1988**, *4*, 31.
(40) Van Krevelen, D. W. *Properties of Polymers*, 3rd ed.; Elsevier Science Publishers B.V.: Amsterdam 1990.
(41) Brandrup, J., Immergut, E. H., Eds. *Polymer Handbook*, 2nd ed.; Wiley-Interscience: New York, 1977.
(42) Zirkel, A.; Urban, V.; Richter, D.; Fetters, L. J.; Huang, J. S.; Kampmann, R.; Hadjichristidis, N. *Macromolecules* **1992**, *25*, 6148.

MA950194G